VILNIUS UNIVERSITY

MYKOLAS JURGIS BILINSKAS

DEVELOPMENT AND APPLICATION OF A MATHEMATICAL MODEL TO PARAMETRIZATION AND REGISTRATION OF BREAST AREA COMPUTED TOMOGRAPHY

Summary of Doctoral Dissertation
Physical Sciences, Informatics (09 P)

Vilnius, 2018

The doctoral dissertation was prepared at Vilnius University in 2013 to 2017.

Scientific Supervisor

Prof. Dr. Habil. Gintautas Dzemyda (Vilnius University, Physical Sciences, Informatics – 09 P).

The defence Council:

Chairman

Prof. Dr. Habil. Antanas Žilinskas (Vilnius University, Physical Sciences, Informatics – 09 P).

Members:

Prof. Dr. Habil. Romualdas Baušys (Vilnius Gediminas Technical University, Technology Sciences, Informatics Engineering – 07 T),

Prof. Dr. Robertas Damaševičius (Kaunas University of Technology, Physical Sciences, Informatics – 09 P),

Prof. Dr. Tomas Krilavičius (Vytautas Magnus University, Physical Sciences, Informatics – 09 P),

Prof. Dr. Alexander Tuzikov (United Institute of Informatics Problems, Belarus, Physical Sciences, Informatics – 09 P).

The dissertation will be defended at the public meeting of the Council of the Scientific Field of Informatics Sciences of Vilnius University in the auditorium number 203 at the Institute of Data Science and Digital Technologies of Vilnius University on 9th February, 2018 at 12:00.

Address: Akademijos St. 4, LT-08412 Vilnius, Lithuania.

The summary of the doctoral dissertation was distributed on the 9th January, 2018.

The dissertation is available at the library of Vilnius University.

VILNIAUS UNIVERSITETAS

MYKOLAS JURGIS BILINSKAS

MATEMATINIO MODELIO SUKŪRIMAS IR TAIKYMAS KRŪTINĖS LĄSTOS KOMPIUTERINĖS TOMOGRAFIJOS VAIZDAMS PARAMETRIZUOTI IR REGISTRUOTI

Daktaro disertacija
Fiziniai mokslai, informatika (09 P)

Vilnius, 2018

Disertacija rengta 2013–2017 metais Vilniaus universitete.

Mokslinis vadovas

prof. habil. dr. Gintautas Dzemyda (Vilniaus universitetas, fiziniai mokslai, informatika – 09 P).

Disertacija ginama viešame Gynimo tarybos posėdyje:

Pirmininkas

prof. habil. dr. Antanas Žilinskas (Vilniaus universitetas, fiziniai mokslai, informatika – 09 P).

Nariai:

prof. habil. dr. Romualdas Baušys (Vilniaus Gedimino technikos universitetas, technologijos mokslai, informatikos inžinerija – 07 T),

prof. dr. Robertas Damaševičius (Kauno technologijos universitetas, fiziniai mokslai, informatika – 09 P),

prof. dr. Tomas Krilavičius (Vytauto Didžiojo universitetas, fiziniai mokslai, informatika – 09 P),

prof. dr. Alexander Tuzikov (Jungtinis informatikos problemų institutas, Baltarusija, fiziniai mokslai, informatika – 09 P).

Disertacija bus ginama viešame Gynimo tarybos posėdyje 2018 m. vasario 9 d. 12 val. Vilniaus universiteto Duomenų mokslo ir skaitmeninių technologijų instituto 203 auditorijoje.

Adresas: Akademijos g. 4, LT-08412 Vilnius, Lietuva.

Disertacijos santrauka išsiuntinėta 2018 m. sausio 9 d.

Disertaciją galima peržiūrėti Vilniaus universiteto bibliotekoje ir VU interneto svetainėje adresu: www.vu.lt/lt/naujienos/ivykiu-kalendorius

1 Introduction

1.1 Research area

Modern technologies allow us to collect a huge amount of data. Finding patterns, trends, and anomalies in these datasets, and summarizing them with simple quantitative models, is one of the grand challenges of the information age: turning data into information and turning information into knowledge. Images are the principal sensory pathway to knowledge about the natural world. A lot of visual data are obtained in medical imaging technologies and every technology needs special methods to be analysed.

The scope of this work is analysis methods of computed tomography images. The slices are registered to find their relative position in the human vertical axis. Only the breast area is considered, – this area is particularly important because many important internal organs are located here: liver, heart, stomach, pancreas, lungs, etc. It is mostly protected by the rib cage.

1.2 Relevance of the Problem

Many diseases may be diagnosed and their treatment observed using the computed tomography (CT), i.e. a technology allowing the inside of objects to be spatially viewed, using computer-processed X-rays. CT scans are 3D images, i.e. a collection of 2D images (slices), representing human body cross-section with a transversal plane. When evaluating the efficiency of treatment or progress of the disease, pre- and post-treatment CT scans must be made (for the same patient). Then radiologists sometimes need to find a position of a single slice of one computed tomography (CT) scan in another scan. The search must be independent of a patient position with respect to bed and the radiocontrast agent injection. The registration problem could be solved by using the metadata of the DICOM header of a CT scan. However, the available information is often error-prone.

1.3 The Aim and Tasks of the Research

The goal of this paper is to reveal a possibility to register a computed tomography slices by the fragments of the rib bone in the slice.

To realize the aim of research, it is necessary to solve the following tasks:

1. To perform an analytical review of medical imaging technologies and image analysis methods, emphasizing the computed tomography and medical image registration.
2. To develop a mathematical model that describes the rib-bounded contour in a computed tomography scan slice, parallel to the transversal human plane.
3. To create an optimization problem to find parameters of the model by the distribution of bone tissue pixels and to propose an algorithm for solving this problem.
4. To develop a method for registration a breast area CT scan slices, based on the mathematical model that approximates the rib-bounded contour.
5. To carry out the experiments on new registration methods and its steps.

1.4 Scientific Novelty

1. A mathematical model that describes the rib-bounded contour in a computed tomography scan slice, parallel to the transversal human plane, has been developed.
2. An optimization problem has been formulated for finding out the parameters of model.
3. The possibility has been proved to register breast area computed tomography scan slices by the rib fragments collocation, described by the mathematical model that approximates the rib-bounded contour.

1.5 Statements to be Defended

1. Breast area computed tomography scan slices can be registered by the rib fragments collocation, described by the mathematical model that approximates the rib-bounded contour.
2. The proposed registration method is invariant to translation, rotation, and scale, therefore slices can be registered independently of the patient position with respect to bed and scanner parameters that determine the size of pixels.

3. The supplementary line segment, parallel to the human sagittal axis, ensures a good approximation of bones near the spine.
4. The possibilities of Pyramidal Implementation of the Lucas-Kanade Feature Tracker are not sufficient for the registration of computed tomography slices.
5. Slice registration is influenced not only by the rib-bounded contour shape, but also by the distribution of bone tissue pixels in the neighbourhood of the model curve points.

1.6 Approbation of the Research

The main results of the dissertation were published in 6 research papers: three papers are published in periodicals, reviewed scientific journals; three papers are published in conference proceedings. The main results have been presented and discussed at 6 national and 4 international conferences.

1.7 Outline of the Dissertation

The dissertation consists of 5 chapters, references, and appendix. The chapters of the dissertation are as follows: Introduction, Review of Medical Imaging Technologies and Image Analysis Methods, Approximation of the Rib-Bounded Contour Using a Mathematical Model, Registration of Computed Tomography Scan Slice, and Conclusions. The dissertation also includes the list of notation and abbreviations. The scope of the work is 120 pages that include 37 figures and 13 tables. The list of references consists of 100 sources.

2 Review of Medical Imaging Technologies and Image Analysis Methods

In the first chapter, medical imaging technologies and medical image analysis methods are reviewed, mostly emphasising computed tomography and tomography image registration methods. General image registration methods are discussed as well, but, since the texture of medical images are not as discriminative as the natural ones, the former need single-purpose methods.

In addition, bone segmentation was also reviewed because it is heavily used for medical image registration. Unfortunately, up till now most of the papers discussing the bone segmentation describe either 3D or projective radiogram segmentation, and to our best knowledge, no attempt to address the segmentation of bones in a single CT slice has found its way to journal publications. One of this work advantages is that it is dedicated to work with a single CT slice.

Several papers, describing rib models and methods for registration of slice with the human atlas, were reviewed because this work can be compared to that papers up to a certain point.

3 Approximation of the Rib-Bounded Contour Using a Mathematical Model

In the second chapter, a method for rib-bounded contour (in the computed tomography scan slice parallel to the human transverse plane) approximation is proposed. This method consists of two steps: bone tissue segmentation and approximating the rib-bounded contour by a mathematical function.

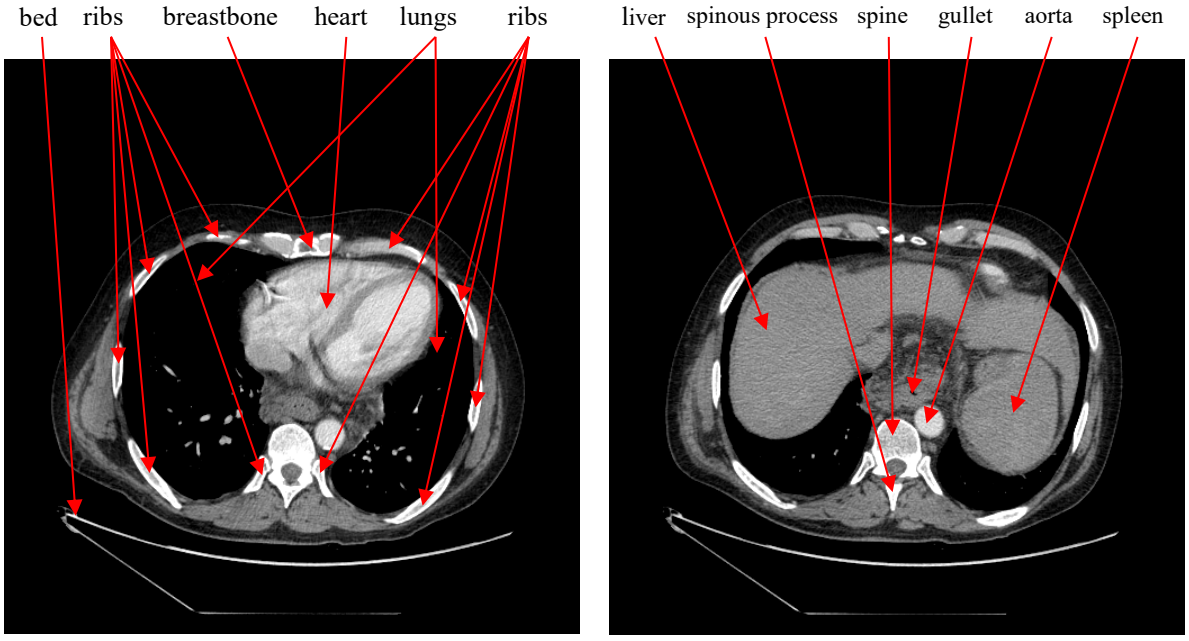

(a) *(b)*

Figure 1. Content of the slices: (a) cross-section through the heart, (b) cross-section through the liver.

In this work, images of size 512×512 are investigated, gathered by GE LightSpeed Pro 32 CT scanner[1]. Figure 1 details the possible content of particular scan slices.

3.1 Segmentation of Ribs, Breastbone, and Spine

The proposed bone tissue segmentation method consists of five steps:

1. Bilateral filtering;
2. Bed segmentation;
3. Dual thresholding;
4. Bloodstream part segmentation;
5. Filtering of outer blobs.

Bilateral filtering is used to avoid a noise after thresholding; the result of the filtering is depicted in Figure 2*(a)*. Bed segmentation is performed by filtering out the blob connected with the bottommost pixel in the slice (here the blob is a connected component of non-zero pixels). Since each CT scan voxel value corresponds to the tissue it reflects (opposite to projectional radiography, where a pixel is the accumulated value of a ray), thresholding is used for segmentation. Here dual thresholding was used with lower and upper thresholds: firstly the upper threshold is used, then the pixels inside holes with the value higher than the lower threshold are added to the segmentation result.

After thresholding the lateral object such as bloodstream parts (if the scan was made with a radio-contrast agent injected; see Figure 2*(b)*) are selected, but all of them lie inside the rib-bounded contour. The greatest problem is that aorta is so close to spine that it looks as connected with the spine. Firstly, the binary image is morphologically eroded by the kernel of radius 7 and distance transform is computed for the eroded image (see Figure 2*(c)*). Then the heart is at the top of the range of interest. Distance transform is computed to find the centre of the aorta. Local maxima greater than 3 and less than 9, and blobs of area smaller than 200 are filtered (if there is no such local maximum, there is no visible aorta in the slice or it is not connected to the spine). The local maximum with the shortest distance between it and the mass centre of blob is the centre of the aorta. When the aorta

[1] http://www3.gehealthcare.com/en/products/categories/goldseal_-_refurbished_systems/goldseal_computed_tomography/goldseal_vct_series

was identified, the medial axis transform of non-eroded binary image is computed (the result is illustrated in Figure 2*(d)*) and the path between aorta centre and spine centre is found in this transform. The spine centre is the nearest local maximum of distance transform from aorta. The circle with the centre at the lowest value point of the path and the radius of that point value separates aorta from spine in the initial binary image.

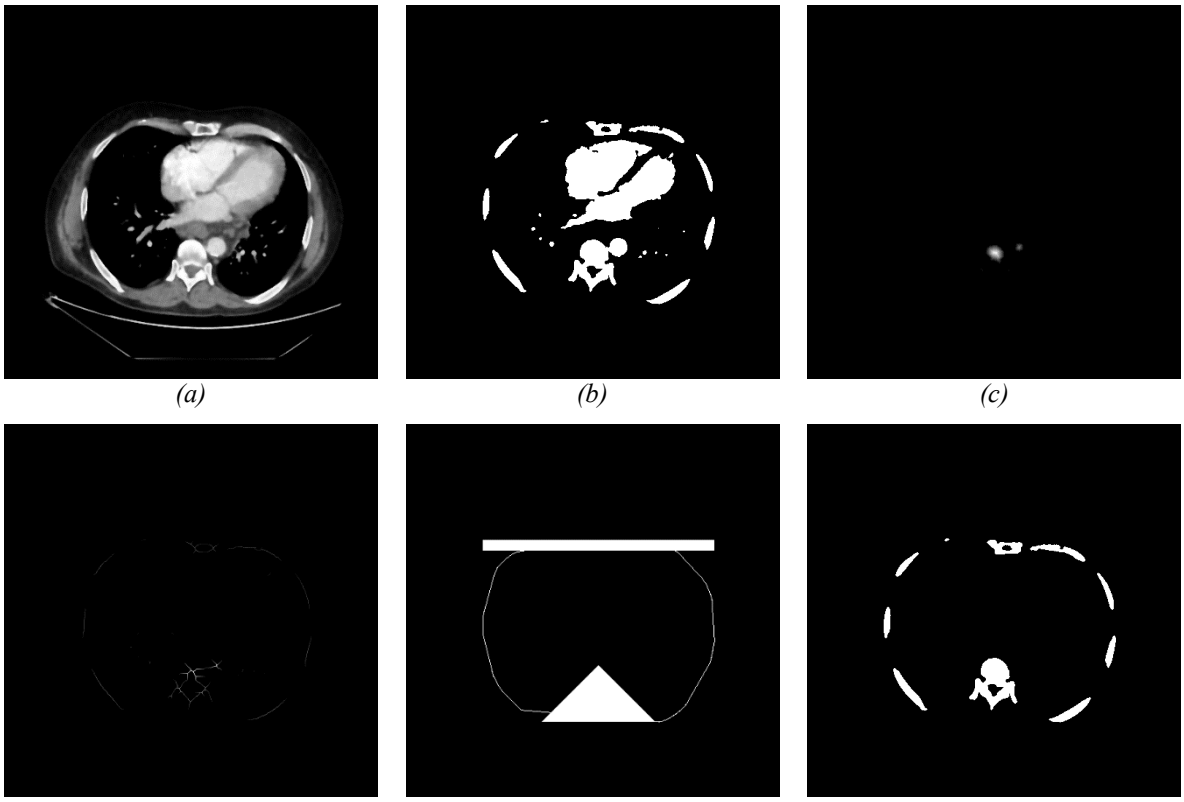

(a) *(b)* *(c)*

(d) *(e)* *(f)*

Figure 2. Bone segmentation: *(a)* a slice after bilateral filtering, *(b)* a binary image after dual thresholding, *(c)* distance transform of the binary image, *(d)* medial axis transform of the binary image, *(e)* seeds for filtering bones, *(f)* final result of segmentation.

Once the aorta is separated from the spine, the bones (ribs, breastbone, and spine) can be segmented by filtering blobs connected with three seeds (see Figure 2*(e)*): a convex hull of the binary image, a triangle for the spine at the bottom, and a strip at the top of the range of interest for the breastbone. The final segmentation result is shown in Figure 2*(f)*; Denote the set of coordinates of bone pixels, obtained during analysis of CT image slices, by $\boldsymbol{B} = \{\boldsymbol{b}_i = [b_{1i} \quad b_{2i}]^\top, i = \overline{1,m}\}$, m is the number of bone pixels. The proposed method does not consider slices with the scapula visible. The C# code of bone segmentation is given in Appendix A of the dissertation.

3.2 The Model Approximating the Rib-Bounded Contour

The ribs form a shape (Figure 1) similar to cardioid:

$$\rho(\varphi) = 1 + \cos(\varphi - \pi/2), \qquad \varphi \in \left[-\frac{\pi}{2}; \frac{3\pi}{2}\right), \tag{1}$$

Here, $\rho(\varphi)$ is a radius and φ is a polar angle. The shape of (1) is depicted in Figure 3 (blue curve). It seems similar, because it features a cave that could be used to approximate the rib cave near the spine. $\pi/2$ is introduced in (1) because the standard cardioid is rotated by $\pi/2$ as compared with Figure 3 and the rib-bounded contour in the images should be oriented just like the ribs depicted in Figure 1.

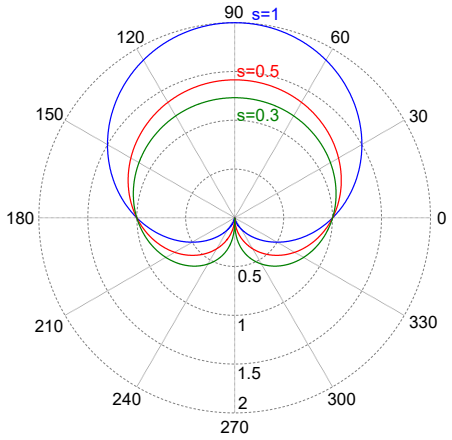

Figure 3. Cardioids: the blue curve is the standard cardioid (1), red and green curves are (2) curves with $s = 0.5$ and $s = 0.3$, respectively.

Figure 1 indicates that the rib-bounded contour is more condensed vertically than the standard cardioid curve. Therefore, we suggest to add an optimizable parameter s:

$$\rho(\varphi) = \left(1 + \cos\left(\varphi - \frac{\pi}{2}\right)\right)^s. \tag{2}$$

The parameter s influences not only the vertical scale of curve (1), but also the form of the curve (see Figure 3 for curves with different values of s).

In the CT scan slice (Figure 1), we see a cave influenced by the breastbone. Curve (2) is convex in this region. Therefore, we need to complement model (2) by an additional member ρ^+ the form of which may vary depending on the cave:

$$\rho(\varphi) = \left(1 + \cos\left(\varphi - \frac{\pi}{2}\right)\right)^s - \rho^+(\varphi). \tag{3}$$

The function $\rho^+(\varphi)$ may be as follows:

$$\rho^+(\varphi) = c\sin^l((\varphi + \pi/2)/2) \tag{4}$$

In (4), we have two control parameters characterizing the breastbone cave for which the optimal values need to be found: l defines the steepness of a curve describing the cave and c is the scale of subtraction.

Moreover, we need some additional parameters a and b that define the horizontal and vertical scales of the curve which approximates the rib-bounded contour, respectively. Curve (3) should be fitted to ribs in the image of bone tissue. Therefore, we need the optimal place for the point of (3) corresponding to $\varphi = 0$ in the image; denote the coordinates of this point by $[x_0 \quad y_0]^\top$.

As we see in Figure 1, the rib-bounded contour has some rotation in respect of the bed. Therefore, we need to introduce the angle θ of such rotation. If the values of s, θ, a, b, x_0, y_0, c, and l are fixed, we can draw a parametric curve $[x \quad y]^\top = [x(\varphi) \quad y(\varphi)]^\top$ approximating the rib-bounded contour:

$$\begin{aligned} x(\varphi) &= x_0 + a\rho(\varphi)\cos\varphi\cos\theta - b\rho(\varphi)\sin\varphi\sin\theta \\ y(\varphi) &= y_0 + a\rho(\varphi)\cos\varphi\sin\theta + b\rho(\varphi)\sin\varphi\cos\theta\,, \end{aligned} \tag{5}$$

where $\rho(\varphi)$ is defined by (3).

While the ribs are symmetric, their cross-section may appear asymmetric due to the position of the patient on the bed. Even more, the spine is a very large white blob in the image of bone tissue, so it can attract one side of the curve. Moreover, we observe a spinous process in the spine bone tissue (see Figure 1 and 2*(f)*). This spinous process influences the shape of the model as well. The notes above lead to the addition of a line segment parallel to the sagittal axis in the model. This line segment must include at least the whole spine in the slice: from $[x_0 \quad y_0]^\top$ to the bottom of the unrotated model (case $\theta = 0$). Formally, the line segment is a part of the line that is bounded by two distinct end points (see Figure 4):

$$\begin{aligned} &1. \quad [x_0 \quad y_0]^\top, \\ &2. \quad \left[x_0 + \left(y_0 - \min_y\right)\sin\theta \quad y_0 - \left(y_0 - \min_y\right)\cos\theta\right]^\top, \end{aligned} \tag{6}$$

where $\min_y$ is the minimal value of y defined by (5) in case $\theta = 0$:

$$\min_{\mathrm{y}} = \min_{\varphi}(y_0 + b\rho(\varphi)\sin\varphi)\,. \tag{7}$$

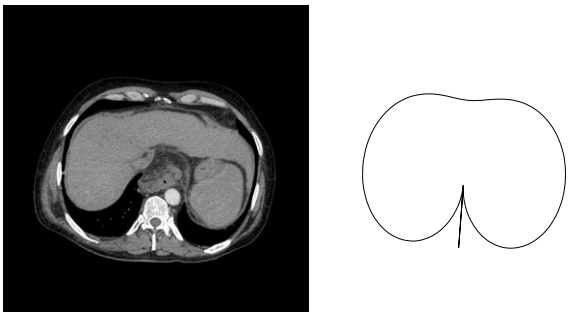

Figure 4. Example of the CT scan slice and a desired model of ribs-contour in this CT slice.

3.2.1 Fitting the Model

If φ runs through the interval $[\pi/2\,;3\pi/2)$ with a step $2\pi/n$, we get the sequence $\boldsymbol{C}^* = \left(\boldsymbol{c}_i^* = [x_i \quad y_i]^\top, i = \overline{0,n-1}\right)$ of curve points, where $x_i = x\left(\frac{2\pi}{n}i - \frac{\pi}{2}\right)$ and $y_i = y\left(\frac{2\pi}{n}i - \frac{\pi}{2}\right)$, $x(\varphi)$ and $y(\varphi)$ are defined by (5). The line segment (6) is sampled by the sequence of n_t points $\boldsymbol{C}^{**} = \left(\boldsymbol{c}_i^{**} = \left[x_0 + \frac{(y_0 - \min_{\mathrm{y}})\sin\theta}{n_t}\cdot i \quad y_0 - \frac{(y_0-\min_{\mathrm{y}})\sin\theta}{n_t}\cdot i\right]^\top, i = \overline{1,n_t}\right)$. Both sequences together form the sequence $\boldsymbol{C} = (\boldsymbol{C}^*, \boldsymbol{C}^{**})$ of the length $n + n_t$.

$\min_{\mathrm{y}}$ is approximated by $\min\limits_{i=\overline{0,n-1}}\left(y_0 + b\rho\left(\frac{2\pi}{n}i - \frac{\pi}{2}\right)\sin\left(\frac{2\pi}{n}i - \frac{\pi}{2}\right)\right)$ to avoid the analytical solving of the equation $\frac{d\rho}{d\varphi}$.

The model of the rib-bounded contour of a particular slice of CT scan has eight parameters the values of which can be varied seeking to find the best approximation of the contour: s, θ, a, b, x_0, y_0, c, and l. The optimal values of these parameters must be defined by the set $\boldsymbol{B} = \left\{\boldsymbol{b}_i = [b_{1i} \quad b_{2i}]^\top, i = \overline{1,m}\right\}$ of coordinates of bone pixels, obtained during the analysis of CT image slices. The optimization problem to find optimal values s, θ, a, b, x_0, y_0, c, and l is formulated as the least squares one:

$$\begin{gathered}\min_{s,c,l,a,b,x_0,y_0,\theta} f(s,c,l,a,b,x_0,y_0,\theta)\,,\\ f(\cdot) = \frac{1}{m}\sum_{i=1}^{m}\left\|\boldsymbol{b}_i - \boldsymbol{c}_{k_i}\right\|^2,\ k_i = \arg\min_{j=0,n+n_t-1}\left\|\boldsymbol{b}_i - \boldsymbol{c}_j\right\|.\end{gathered} \tag{8}$$

Several constraints were used for optimization:

1. $-\pi/6 < \theta < \pi/6$,
2. $y_0 \geq p + \omega$, where p is an ordinate of the upper spine point ($p \in \{b_{2i}\}, i = \overline{1, m}$) in the slice, ω is a constant,
3. $0 \leq c < 1$,
4. $\max_{\varphi}(2a\rho(\varphi)\cos\varphi) > \max_{\varphi}(b\rho(\varphi)\sin\varphi) - \min_{\varphi}(b\rho(\varphi)\sin\varphi)$.

3.2.2 Two-Step Optimization

The direct optimization is not very stable, the problem can be solved by dividing computations into two steps (despite the fact that the function $f(\cdot)$ is not separable):

- the model is fitted without a breastbone cave (s, a, b, x_0, y_0, and θ are variables, while the values of c and l are fixed),
- correction of the model taking into account the breastbone cave.

The first sub problem is simpler as compared to (8), with a smaller number of variables:

$$\min_{s,a,b,x_0,y_0,\theta} f(s, 0{,}2, a, b, x_0, y_0, \theta)\,. \tag{9}$$

As a result, the optimal values of s, a, b, x_0, y_0, and θ are obtained. Six values serve as the starting ones in the second sub-problem that is defined by (8). The sub-problem has two new variables c and l. Their values were fixed in the first sub-problem to be equal to $c = 0$ and $l = 2$. These values were set as the initial ones for variables c and l of the second sub-problem. Some curve fitting examples are illustrated in Figure 5.

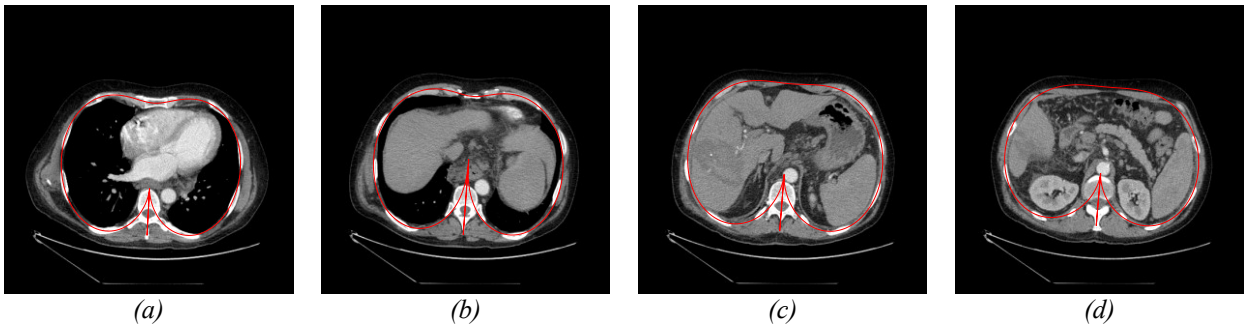

(a) *(b)* *(c)* *(d)*

Figure 5. Examples of curve fitting

In the dissertation, it is shown that the two-step optimization ensures near global minimum, as well as the possibility to speed-up the optimization process was discussed using partial derivatives of the optimized function.

4 Registration of Computed Tomography Scan Slices

Radiologists need to find the position of a slice of one CT scan in another scan. Formally, having a slice A' of scan $\boldsymbol{A'}$, we should compare it with all the slices in scan $\boldsymbol{A''}$ and find the most similar slice A''_k, i.e. the nearest slice from scan $\boldsymbol{A''}$ to A':

$$k = \arg \min_{A''_j \in \boldsymbol{A''}} dist\left(A', A''_j\right), \tag{10}$$

where the function $dist$ is a similarity measure of two slices. Some possible functions $dist$ are discussed below.

All source objects are denoted by one apostrophe, all target objects are denoted by two apostrophes, e. g. A' and $\boldsymbol{A'}$ are called a source or a reference slice and scan, respectively; A'' and $\boldsymbol{A''}$ are called a target slice and scan, respectively.

The registration method below is translation, rotation, and scale invariant. The comparison of slices is based on:

1. The values of parameters describing the model $M = \langle s, c, l, a, b, x_0, y_0, \theta \rangle$;
2. The sequence $\boldsymbol{C}$ of discrete points of the curve of the model;
3. The weights $\boldsymbol{W}$ of points of the curve (optionally);

The length of the sequence $\boldsymbol{C}$ is n because the second part of the model (a line segment) is not used here. Weights $\boldsymbol{W}$ are gathered by distributing bone tissue points among the curve points $[x_i \quad y_i]^\top, i = \overline{0, n-1}$. n groups of bone tissue points are formed. Model points have weights $\boldsymbol{W} = (w_0, w_1, \dots, w_{n-1})$, where w_i is the number of bone tissue points in the ith group; the ith group contains points closer to the model point $[x_i \quad y_i]^\top$ than $[x_j \quad y_j]^\top, \forall j \neq i$. Without loss of generality, further we use $\boldsymbol{W} = (w_0, w_1, \dots, w_{n-1})$ as normalized weights, where $\sum_{i=0}^{n-1} w_i = 1$.

4.1 Registration Invariance

4.1.1 Rotation Invariance

The mathematical model has a parameter θ, describing the rotation of a patient with respect to the bed. This parameter indicates the rotation of the model curve around the point $[x_0 \quad y_0]^\top$ as well. Rotation invariance is realized rotating back the model curve around the point $[x_0 \quad y_0]^\top$ by the angle $-\theta$. This procedure should be applied both to source and target slices. The revised parameters of the models become $M' = \langle s', c', l', a', b', x_0', y_0', 0\rangle$ and $M'' = \langle s'', c'', l'', a'', b'', x_0'', y_0'', 0\rangle$. Without loss of generality and seeking for simplicity of notation, $\boldsymbol{C}$ is redefined by the sequence of points after the rotation described above. Therefore, in the further text, the sequences after rotations of source and target slices are denoted as $\boldsymbol{C}' = ([x_i' \quad y_i']^\top, i = \overline{0, n-1})$ and $\boldsymbol{C}'' = ([x_i'' \quad y_i'']^\top, i = \overline{0, n-1})$, respectively.

4.1.2 Scale Invariance

Most often, the compared CT scan slices have a different scale, i.e. the size of the pixel in millimetres. The scale depends on the parameters of CT scanner. These parameters may vary in different scans. In this work, only quadratic pixels are considered. Three options O1, O2, and O3 of the unification of scales are considered below. Options O2 and O3 are used when DICOM metadata tags are not precise or are even lost.

The first option O1 is the usage of DICOM metadata tags, indicating the size of pixel. Denote the size of the source slice pixel by z' and that of the target slice pixel by z''. The revised parameters of the source slice model are $M' = \langle s', c', l', a' \cdot z'/z'', b' \cdot z'/z'', x_0', y_0', 0\rangle$. The parameters of the target slice remain unchanged.

Options O2 and O3 specify scaling using the following features:

- O2, – the maximal width of the region, bounded by the curve,
- O3, – the area of the region, bounded by the curve.

If the maximal width is considered (O2), then the target slice model remains as it is, and the parameters of the source slice model are revised as follows:

$$M' = \langle s', c', l', a' \cdot z, b' \cdot z, x_0', y_0', 0 \rangle,$$
$$z = width(\boldsymbol{C}'')/width(\boldsymbol{C}'), \tag{11}$$
$$width(\boldsymbol{C}') = \max_i x_i' - \min_i x_i', width(\boldsymbol{C}'') = \max_i x_i'' - \min_i x_i''.$$

If the area of the region bounded by the curve is considered (O3), then the parameters of the source slice model are revised as follows:

$$M' = \langle s', c', l', a' \cdot z, b' \cdot z, x_0', y_0', 0 \rangle,$$
$$z = \sqrt{area(\boldsymbol{C}'')/area(\boldsymbol{C}')}, \tag{12}$$
$$area(\boldsymbol{C}) = \frac{1}{2}(x_0 y_1 - x_1 y_0 + x_1 y_2 - x_2 y_1 + \cdots + x_{n-2} y_{n-1} - x_{n-1} y_{n-2} + x_{n-1} y_0 - x_0 y_{n-1}),$$

Without loss of generality and seeking for simplicity of notation, we redefine $\boldsymbol{C}$ by the sequence of points after scaling described above.

4.1.3 Translation Invariance

There are several reasons generating the necessity to solve the problem of translation invariance. The patient lies in various positions on the bed during different scans, and models corresponding to target and source slices differ, as usual. The translation invariance can be realized in two steps: horizontal translation and the following vertical translation.

The models of bone tissue of the source and target slices have a vertical symmetry: the axis of symmetry crosses the abscissa axis at x_0' and x_0'' for the source and target slices, respectively. The horizontal translation invariance will be ensured by moving the source slice model as follows:

$$\Delta x = x_0'' - x_0'. \tag{13}$$

Note that $x_0'' - x_0' = \frac{1}{n}\sum_{i=0}^{n-1}(x_i'' - x_i')$. The model, corresponding to the source slice, becomes $M' = \langle s', c', l', a' \cdot z, b' \cdot z, x_0' + \Delta x, y_0', 0 \rangle$. The problem is more complicated to find optimal Δy to move the source slice model vertically. The model curve is not symmetric to any horizontal line and the 'spike' of the model may have a different length $(y_0 - \min_i y_i)$ as $\theta = 0$: even similar slices can have a large difference of y_0, because the parameter s may slightly compensate it.

Several strategies for finding Δy are developed and examined below:

Pointwise comparison (PW):

$$\Delta y = \frac{1}{n}\sum_{i=0}^{n-1}(y_i'' - y_i'), \tag{14}$$

Total least-squares (TLS):

The problem to search for optimal Δy may be formulated as total least-squares:

$$\min_{\Delta y}\phi(\Delta y) = \sum_{i=0}^{n-1}\left(y_i'' - (\bar{y}'(x_i'', y_i'', \Delta x, \Delta y) + \Delta y)\right)^2, \tag{15}$$

where $\bar{y}'(x_i'', y_i'', \Delta x, \Delta y)$ is a function giving the ordinate of the nearest point on the source model curve (shifted by $[\Delta x \quad \Delta y]^\mathsf{T}$) from $[x_i'' \quad y_i'']^\mathsf{T}$. In this work, the source model curve was linearly interpolated between the n sampled points, and problem (15) was solved using one-dimensional search.

Weighted total least squares (WTLS):

$$\begin{aligned}\min_{\Delta y}\phi(\Delta y) = \sum_{i=0}^{n-1}\Big(&\left(y_i'' - (\bar{y}'(x_i'', y_i'', \Delta x, \Delta y) + \Delta y)\right)^2 \\ &\cdot \left(w_i'' - \bar{w}'(x_i'', y_i'', \Delta x, \Delta y)\right)^2\Big),\end{aligned} \tag{16}$$

where $\bar{w}'(x_i'', y_i'', \Delta x, \Delta y)$ is a function the value of which is the weight of the nearest point on the source model curve (shifted by $[\Delta x \quad \Delta y]^\mathsf{T}$) from $[x_i'' \quad y_i'']^\mathsf{T}$. In this work, the weights $\bar{w}'(x_i'', y_i'', \Delta x, \Delta y)$ of the source model are linearly interpolated between the sampled points, and problem (16) was solved using one-dimensional search.

Weighted ordinary least squares (WOLS):

$$\Delta y = \frac{\sum_{i=0}^{n-1}\left(y_i'' - \bar{\bar{y}}'(x_i'', \Delta x)\right)w_i'' \cdot \bar{\bar{w}}'(x_i'', \Delta x)}{\sum_{i=0}^{n-1} w_i'' \cdot \bar{\bar{w}}'(x_i'', \Delta x)}, \tag{17}$$

where $\bar{\bar{y}}'(x_i'', \Delta x)$ is a function the value of which is the ordinate of the source model curve (shifted by Δx) at the abscissa point x_i'', dependently on the fact whether the ith point $[x_i'' \quad y_i'']^\mathsf{T}$ of the target model is on top or bottom of the model curve; $\bar{\bar{w}}'(x_i'', \Delta x)$ is the weight of the point of the source model curve (shifted by Δx) at the abscissa point x_i'',

dependently on the fact whether the ith point $[x_i'' \quad y_i'']^\top$ of the target model is on top or bottom of the model curve. In this work, the functions $\bar{\bar{y}}'(x_i'', \Delta x)$ and $\bar{\bar{w}}'(x_i'', \Delta x)$ were obtained by linearly interpolating the source model between the sampled points.

Pyramidal Implementation of the Lucas-Kanade Feature Tracker (LKFT):

Pyramidal Implementation of the Lucas-Kanade Feature Tracker can find features and match them, and the RANSAC method can estimate the transformation matrix. It is realized by the `estimateRigidTransform` function of OpenCV library[2]. This function is applied to two slices (grayscale images) and the estimated transformation matrix can be applied either to a set of bone tissue pixels of the source slice (denote the result by $\boldsymbol{B}^*$) or to the source model curve $\boldsymbol{C}$ (after the weights are estimated). Lucas-Kanade Feature Tracker is used in this work to evaluate the effectiveness of the proposed mathematical model.

4.2 Slice Comparison Criteria

Five slice comparison criteria are proposed.

$$dist(A'; A'') = \sum_{i=0}^{n-1} \left(\left(x_i'' - (x_i' + \Delta x) \right)^2 + \left(y_i'' - (y_i' + \Delta y) \right)^2 \right) \tag{18}$$

is the sum of squared distances between the corresponding source and target points of the model curve in Eq. (10).

$$\begin{aligned} dist(A'; A'') = \sum_{i=0}^{n-1} \Big(& \left(x_i'' - (\bar{x}'(x_i'', y_i'', \Delta x, \Delta y) + \Delta x) \right)^2 \\ & + \left(y_i'' - (\bar{y}'(x_i'', y_i'', \Delta x, \Delta y) + \Delta y) \right)^2 \Big), \end{aligned} \tag{19}$$

where $\bar{x}'(x_i'', y_i'', \Delta x, \Delta y)$ is a function the value of which is an abscissa of the nearest point on the source model curve (shifted by $[\Delta x \quad \Delta y]^\top$) from $[x_i'' \quad y_i'']^\top$.

[2] opencv.org

$$dist(A';A'') = \sum_{i=0}^{n-1} \Big(\Big(\big(x_i'' - (\bar{x}'(x_i'', y_i'', \Delta x, \Delta y) + \Delta x)\big)^2 + \big(y_i'' - (\bar{y}'(x_i'', y_i'', \Delta x, \Delta y) + \Delta y)\big)^2 \Big) \cdot \big(w_i'' - \bar{w}'(x_i'', y_i'', \Delta x, \Delta y)\big)^2 \Big). \quad (20)$$

Slices could be compared according to weights only:

$$dist(A';A'') = \sum_{i=0}^{n-1} \big(w_i'' - \bar{w}'(x_i'', y_i'', \Delta x, \Delta y)\big)^2 . \quad (21)$$

To evaluate the effectiveness of the proposed mathematical model, the registration was performed with a slice comparison criterion that does not use a mathematical model at all, but compares the intersection of bone tissue pixels instead:

$$dist(\boldsymbol{B}^*, \boldsymbol{B}'') = (|\boldsymbol{B}^*| - |\boldsymbol{I}| + |\boldsymbol{B}''| - |\boldsymbol{I}|)/(|\boldsymbol{B}^*| + |\boldsymbol{B}''|) , \quad (22)$$

where $\boldsymbol{B}^*$ is a transformed set $\boldsymbol{B}'$, $\boldsymbol{I}$ is the intersection of $\boldsymbol{B}^*$ and $\boldsymbol{B}''$, $|\cdot|$ is the cardinality of the set. Here the intersection is assumed as a pixel-wise logical AND operator of two binary images $\boldsymbol{B}^*$ and $\boldsymbol{B}''$. The numerator of (22) could be treated as the pixel-wise XOR operator. The function $dist(\boldsymbol{B}^*, \boldsymbol{B}'')$ obtains values from the interval $[0; 1]$. $\boldsymbol{B}'$ could be transformed to $\boldsymbol{B}^*$ using the transformation matrix obtained in the LKFT translation invariance strategy.

4.3 Experiments

The experiments were carried out to find out the best invariance strategy and the slice comparison criterion, as well as what is the influence of slice thickness on the registration results, and the influence of optimization accuracy on the registration error. To evaluate the registration results, scans with the known shifts were registered and the registration error is treated as the absolute distance between two target slice positions of the human vertical axis: obtained by (10) and the correct position.

The Matlab quasi-Newton method was used for optimizing, and the function tolerance $\Delta f(\cdot)$ of 10^{-10} was chosen as a stopping criterion. n was set $n = 180$ and $n_t = 10$.

4.3.1 Evaluation of Slice Comparison Criteria

Since the CT scan slice thickness usually differs and it may impact on registration results, slice comparison criteria were tested by one pair of CT scans, the slice thickness of which is 1,25 mm, the source CT scan has 96 slices, and the target scan has 106 slices. Each comparison criterion was tested using all the options of scale invariances and all the strategies of translation invariances. The registration results were aggregated from 96 slices and expressed by the mean error ε_{mean} (millimetres), the error standard deviation σ, and the maximum error ε_{max} (millimetres), presented in Tables 1-4. The seeking mean error must be no more than half the slice thickness of a target slice, in this case, $\varepsilon_{mean} \leq 0{,}625$.

Table 1. Registration results obtained using (18).

	PW			TLS			WTLS			WOLS		
	ε_{mean}	σ	ε_{max}	ε_{mean}	σ	ε_{max}	ε_{mean}	σ	ε_{max}	ε_{mean}	σ	ε_{max}
O1	6,58	8,41	36,3	7,10	9,42	46,3	6,47	8,49	36,3	4,53	4,84	26,3
O2	8,88	11,5	47,5	9,30	11,8	47,5	9,22	12,1	46,3	5,42	5,92	26,3
O3	9,96	12,8	56,3	9,23	11,7	47,5	9,52	12,7	56,3	5,14	5,64	26,3

Table 2. Registration results obtained using (19).

	PW			TLS			WTLS			WOLS		
	ε_{mean}	σ	ε_{max}	ε_{mean}	σ	ε_{max}	ε_{mean}	σ	ε_{max}	ε_{mean}	σ	ε_{max}
O1	7,24	9,22	38,8	9,97	9,23	38,8	9,92	9,47	38,8	6,9	5,39	25,0
O2	8,63	11,9	46,3	10,1	14,6	60,0	11,3	15,5	60,0	4,15	4,73	26,3
O3	7,72	10,9	46,3	8,74	13,5	60,0	9,17	13,7	60,0	4,99	5,32	31,3

Table 3. Registration results obtained using (20).

	PW			TLS			WTLS			WOLS		
	ε_{mean}	σ	ε_{max}	ε_{mean}	σ	ε_{max}	ε_{mean}	σ	ε_{max}	ε_{mean}	σ	ε_{max}
O1	0,68	0,76	2,50	1,17	1,41	12,5	0,98	0,60	2,50	0,85	0,69	2,50
O2	0,76	0,87	3,75	0,86	1,24	6,25	0,47	0,66	2,50	0,49	0,69	3,75
O3	0,74	0,86	3,75	0,94	1,22	6,25	0,70	0,74	3,75	0,64	0,67	2,50

Table 4. Registration results obtained using (21).

	PW			TLS			WTLS			WOLS		
	ε_{mean}	σ	ε_{max}	ε_{mean}	σ	ε_{max}	ε_{mean}	σ	ε_{max}	ε_{mean}	σ	ε_{max}
O1	0,44	0,67	2,5	0,57	0,76	3,75	0,47	0,61	1,25	0,51	0,61	1,25
O2	0,29	0,53	1,25	0,43	0,69	3,75	0,31	0,54	1,25	0,33	0,55	1,25
O3	0,23	0,52	2,5	0,33	0,55	1,25	0,26	0,51	1,25	0,34	0,56	1,25

The results in Tables 3 and 4 show that the methods using weights achieve better results by one row as compared to results obtained by methods without using weights (Tables 1 and 2).

4.3.2 Influence of Slice Thickness on the Registration Results

The registration results of CT scans with different slice thickness are presented in Table 5 using O2 scale invariance, WOLS translation invariance, and slice comparison criterion (21). Column *(a)* refers to the source slice thickness, *(b)* refers to the target slice thickness, *(c)* refers to the count of source slices (the results are aggregated from this amount of slices), and *(d)* refers to the count of target slices. Each row describes the results of registration of one pair of scans. Note that the results in the first row coincide with the results in Table 4, O2 row, WOLS group.

Table 5. Registration results of CT scans with different slice thickness.

(a)	*(b)*	*(c)*	*(d)*	ε_{mean}	σ	ε_{max}
1,25	1,25	96	106	0,326	0,549	1,25
2,5	1,25	48	106	0,156	0,413	1,25
2,5	1,25	49	106	0	0	0
2,5	2,5	49	53	0,102	0,495	2,5
1,25	2,5	103	53	0,121	0,537	2,5
1,25	2,5	106	53	0,142	0,578	2,5

Table 5 does not indicate a clear relation of registration results with slice thickness. It is because a thicker slice is not so similar to the neighbouring slices, so the errors are less frequent, but the significance of one error is higher.

4.3.3 Slice registration using Pyramidal Lucas-Kanade Feature Tracker

The registration results of CT scans with different slice thickness are presented in Table 6 using Pyramidal Implementation of the Lucas-Kanade Feature Tracker. Columns *(a)-(d)* and rows are analogous to that in Table 5.

Table 6. Registration results obtained using LKFT.

				Criterion (22)			Criterion (21)		
(a)	*(b)*	*(c)*	*(d)*	ε_{mean}	σ	ε_{max}	ε_{mean}	σ	ε_{max}
1,25	1,25	96	106	1,00	0,91	3,75	1,95	4,03	38,8
2,5	1,25	48	106	0,60	0,67	2,50	4,66	10,2	40,0
2,5	1,25	49	106	0,43	0,74	2,50	2,12	5,52	38,8
2,5	2,5	49	53	0,61	1,08	2,50	3,01	5,71	40,0
1,25	2,5	103	53	0,34	0,86	2,50	1,84	1,84	7,50
1,25	2,5	106	53	0,33	0,85	2,50	4,58	10,6	45,0

The results in Table 6 show the importance of slice alignment, because it is possible to compare the slice with different criteria, while the transformation invariance plays the key role. Pyramidal Implementation of the Lucas-Kanade Feature Tracker makes small errors estimating the transformation matrix, but these small errors imply large errors in the final registration. Also this tracker is not suitable to align slices with different radio-contrast agent injection.

4.3.4 Influence of Optimization Accuracy on the Registration Error

To evaluate the influence of the optimization stopping criterion and count n of the model curve points on the registration accuracy, the experiments were carried out using a pair of CT scans with different n and different $\Delta f(\cdot)$. O2 scale invariance, WOLS translation invariance strategies, and (21) slice comparison criterion were used. In Table 7, the registration results are given, the columns are grouped by the optimization stopping criterion, and rows represent the results with different n.

Table 7. Influence of optimization accuracy on the registration error.

n	$\Delta f(\cdot) < 10^{-4}$			$\Delta f(\cdot) < 10^{-6}$			$\Delta f(\cdot) < 10^{-8}$			$\Delta f(\cdot) < 10^{-10}$		
	ε_{mean}	σ	ε_{max}	ε_{mean}	σ	ε_{max}	ε_{mean}	σ	ε_{max}	ε_{mean}	σ	ε_{max}
30	1,38	3,19	30	0,96	1,13	5,0	0,96	0,98	3,75	0,96	0,98	3,75
45	1,47	7,85	77,5	1,46	7,85	77,5	1,43	7,85	77,5	1,43	7,85	77,5
60	0,52	0,67	2,5	0,57	0,7	2,5	0,55	0,72	3,75	0,55	0,72	3,75
90	0,65	0,74	2,5	0,56	0,74	2,5	0,57	0,74	2,5	0,57	0,74	2,50
180	0,34	0,58	2,5	0,38	0,63	2,5	0,34	0,56	1,25	0,34	0,56	1,25

In every case of Table 7, a computation time for curve fitting to each slice of two CT scans (206 slices in total) is evaluated. The time is presented in Table 8. The optimization was carried out by a computer with Intel® Core™ i7-2600 @ 3,4GHz and Matlab R2013a. In Table 9, a computation time of the registration is presented.

Table 8. Computation time of the optimization.

n	$\Delta f(\cdot) < 10^{-4}$	$\Delta f(\cdot) < 10^{-6}$	$\Delta f(\cdot) < 10^{-8}$	$\Delta f(\cdot) < 10^{-10}$
30	497978	520933	529558	524893
45	534591	562763	584072	585623
60	686761	743194	755061	757077
90	1008763	1097189	1132819	1134220
180	1980107	2184475	2264490	2261621

Table 9. Computation time of the registration.

n	$\Delta f(\cdot) < 10^{-4}$	$\Delta f(\cdot) < 10^{-6}$	$\Delta f(\cdot) < 10^{-8}$	$\Delta f(\cdot) < 10^{-10}$
30	390	703	359	281
45	453	671	984	62
60	734	656	750	593
90	437	859	453	859
180	531	828	656	187

The registration results seem to be sensitive to the count n of model curve points. For larger n a softer optimization accuracy $\Delta f(\cdot)$ could be chosen. In every case the best results are achieved with $n = 180$.

5 Conclusions

1. The proposed mathematical model that approximates the rib-bounded contour in a CT scan slice parallel to the human transverse axis, is also capable to evaluate patient rotation around the vertical axis during the scan.
2. The distribution of bone tissue pixels is dense near the spine and it can influence the general form of the model. The supplementary line segment, parallel to the human sagittal axis, ensures good bone approximation near the spine.
3. The two-step optimization was proposed to evaluate the values of parameters of the model: in the first step, a simplified problem is solved, in the second step, the full problem is solved. The experiments shows that global optimization problem can be solved using local optimization methods.
4. The proposed registration method is invariant to translation, rotation, and scaling, therefore CT scan slices could be registered independently of a patient position with respect to the bed and the parameters of the scanner that determine the size of pixels. $\sim 0{,}1$ mm average registration error was achieved.
5. The experiments have shown that the transformation matrix, obtained using pyramidal implementation of the Lucas-Kanade Feature Tracker, is not suitable for source slice transformation because a small error of transformation matrix causes a large error in the final registration result. Using this method the achieved average error was 1 mm and the maximum error was $3{,}75$ mm, while the best achieved average and maximum error was $0{,}33$ mm and $1{,}25$ mm, respectively, with the same data.
6. Four different translation invariance strategies and three scale invariance options have been tested. The best results were achieved when not only the shape of the rib-bounded contour, but also the distribution of bone tissue pixels in the neighbourhood of the model curve points are considered. Methods that uses weights yielded better results by one row as compared with methods without using weights.

6 List of Publications on the Topic of Dissertation

1. **Mykolas J. Bilinskas**, Gintautas Dzemyda, Mantas Trakymas. Approximation of the Ribs-Bounded Contour in a Tomography Scan Slice. *International Journal of Information Technology & Decision Making*, 2017, ISSN 0219-6220. Accepted, 10.1142/S0219622017500298. (IF 2016: 1,664).
2. **Mykolas J. Bilinskas**, Gintautas Dzemyda, Martynas Sabaliauskas. Speeding-up the Fitting of the Model Defining the Ribs-bounded Contour. *Applied Computer Systems*, **21**(1), 2017, ISSN 2255-8691, p. 66–70.
3. **Mykolas J. Bilinskas**, Gintautas Dzemyda, Mantas Trakymas. Feature-Based Registration of Thorax CT Scan Slices. *Informatica*, **28**(3), 2017, ISSN 0868-4952, p. 439-452. 10.15388/Informatica.2017.137. (IF 2016: 1,056).

About the author

Mykolas J. Bilinskas received a Bachelor‘s degree (in 2011 m.) and a Master‘s degree (in 2013 m.) in Informatics from Vilnius University. He completed the Master‘s studies with an honours „Cum Laude“ diploma for his academic achievements. From 2013 to 2017 he was a PhD student at Vilnius University. He worked for the European Organization of Nuclear Research (CERN, Switzerland) as an intern during the summer of 2009. His industrial experience includes programming at „Altechna R&D“ (Vilnius) in 2012.

Matematinio modelio sukūrimas ir taikymas krūtinės ląstos kompiuterinės tomografijos vaizdams parametrizuoti ir registruoti

1 Tyrimų sritis

Šiame darbe nagrinėjami kompiuterinės tomografijos vaizdai ir jų analizės metodai efektyviai paciento stebėsenai ir diagnostikai, taikant daugkartinę tomografiją, pasiekti. Ypač daug dėmesio skirta šonkauliais ribojamos srities vaizdų registravimui. Vaizdų registravimu įvardijamas procesas, kai skirtingi vaizdai transformuojami į vieną koordinačių sistemą. Vaizdų registravimo taikymas yra itin platus, jis yra būtinas norint palyginti ar sujungti vaizdus, gautus skirtingu metu, skirtingais įrenginiais ar skirtingais įrenginių nustatymais. Medicinoje vaizdų registravimas yra svarbus, kai atliekami kompiuterinės tomografijos tyrimai prieš ir po gydymo, ir siekiant įvertinti gydymo efektyvumą reikia palyginti šių tyrimų vaizdus ar atskirus jų sluoksnius. Šiame darbe lyginami sluoksniai siekiant įvertinti jų padėtį žmogaus vertikalioje ašyje.

2 Darbo aktualumas

Tam tikros ligos gali būti diagnozuotos ir jų gydymas stebimas naudojant kompiuterinę tomografiją (CT), kuri leidžia pamatyti objektų vidų rentgeno spinduliais. Tomografiniai vaizdai yra trimačiai rastriniai vaizdai: dvimačių rastrinių vaizdų – sluoksnių – rinkinys. Sluoksnis vaizduoja kūno skerspjūvį pagal plokštumą, lygiagrečią skersinei žmogaus plokštumai. Tomografiniai vaizdai daromi tam pačiam pacientui įvairiais gydymo laikotarpiais, taip pat su kontrastinėmis medžiagomis ir be jų. Tai leidžia be chirurginės intervencijos stebėti žmogaus organizmo pokyčius ir pasirinkti tinkamą gydymo strategiją. Dažnas kompiuterinės tomografijos objektas yra krūtinės sritis, ji ypatinga tuo, kad turi daug svarbių vidinių organų: skrandis, širdis, plaučiai, kepenys, kasa ir kt., o juos saugo šonkauliai.

Medikai susiduria su uždaviniu surasti vieno tomografinio vaizdo sluoksnio poziciją kitame tomografiniame vaizde. Sluoksnių registravimas turi nepriklausyti nuo paciento pozicijos lovos atžvilgiu ar kontrastinės medžiagos. Ši problema galėtų būti išspręsta

trivialiai pagal DICOM meta duomenis, tačiau šie metaduomenys yra netikslūs arba išvis klaidingi, todėl reikia ieškoti naujų tomografinių vaizdų sluoksnių registravimo būdų.

3 Darbo tikslas ir uždaviniai

Darbo tikslas – atskleisti galimybę registruoti krūtinės srities kompiuterinės tomografijos vaizdų sluoksnius pagal šonkaulių fragmentų išsidėstymą.

Tikslui pasiekti sprendžiami šie uždaviniai:

1. Atlikti analitinę medicininių vaizdų analizės metodų ir technologijų apžvalgą, išskirtinį dėmesį skiriant kompiuterinei tomografijai ir medicininių vaizdų registravimui.
2. Sukurti matematinį modelį, aproksimuojantį šonkauliais ribojamą sritį kompiuterinės tomografijos vaizdo sluoksnyje, lygiagrečiame žmogaus skersinei plokštumai.
3. Suformuluoti optimizavimo uždavinį modelio parametrų reikšmėms nustatyti pagal kaulinio audinio pikselių išsidėstymą kompiuterinės tomografijos vaizdo sluoksnyje ir pasiūlyti algoritmus tam uždaviniui spręsti.
4. Sukurti krūtinės srities CT vaizdų sluoksnių registravimo pagal šonkaulių fragmentų išsidėstymą metodą, kuris remtųsi matematiniu modeliu, aproksimuojančiu šonkauliais ribojamą sritį.
5. Atlikti eksperimentinį naujo registravimo metodo ir jo atskirų etapų tyrimą.

4 Mokslinis naujumas

1. Sukurtas matematinis modelis, aproksimuojantis šonkauliais ribojamą sritį kompiuterinės tomografijos vaizdo sluoksnyje, lygiagrečiame žmogaus skersinei plokštumai.
2. Suformuluotas optimizavimo uždavinys pasiūlyto modelio parametrams nustatyti.
3. Įrodyta galimybė krūtinės ląstos CT vaizdų sluoksnius registruoti pagal šonkaulių fragmentų išsidėstymą, aprašomą matematiniu modeliu, aproksimuojančiu šonkauliais ribojamą sritį.

5 Ginamieji teiginiai

1. Krūtinės ląstos CT vaizdų sluoksnius galima registruoti pagal šonkaulių fragmentų išsidėstymą, aprašomą matematiniu modeliu, aproksimuojančiu šonkauliais ribojamą sritį.
2. Pasiūlytas registravimo metodas yra invariantiškas poslinkiui, posūkiui ir mastelio pokyčiui, todėl sluoksnius galima registruoti nepriklausomai nuo paciento pozicijos lovos atžvilgiu ir tomografo parametrų, lemiančių pikselio dydį.
3. Modelio papildymas atkarpa, lygiagrečia žmogaus sagitalinei ašiai, užtikrina gerą šonkaulių sistemos aproksimaciją ir stuburo aplinkoje.
4. Piramidinio Lucas-Kanade algoritmo teikiamos galimybės nėra pakankamos kompiuterinės tomografijos vaizdams registruoti.
5. Sluoksnių registravimui įtaką daro ne tik šonkauliais apriboto kontūro forma, o ir kaulinį audinį vaizduojančių pikselių tankis modelio kreivės taškų aplinkoje.

6 Disertacijos struktūra

Disertaciją sudaro 5 skyriai ir literatūros sąrašas. Disertacijos skyriai: Įvadas, Mediciniių vaizdų analizės metodų ir technologijų apžvalga, Šonkauliais apriboto kontūro aproksimavimas matematiniu modeliu, Sluoksnių registravimas ir Išvados. Be to, disertacijoje pateikti paveikslų, lentelių, naudotų žymėjimų ir santrumpų sąrašai. Visa disertacijos apimtis yra 120 puslapių, pateikti 37 paveikslai ir 13 lentelių. Disertacijoje remtasi 100 literatūros šaltinių.

7 Išvados

1. Pasiūlytas matematinis modelis, aproksimuojantis šonkaulių skerspjūvį kompiuterinės tomografijos vaizdo sluoksnyje, lygiagrečiame žmogaus skersinei plokštumai, leidžia ir įvertinti paciento posūkį pagal vertikalią ašį tomografijos atlikimo metu.
2. Kaulinį audinį vaizduojančių pikselių tankis ypač didelis stuburo aplinkoje, tad ši vieta gali paveikti bendrą modelio struktūrą. Atkarpos, lygiagrečios žmogaus

sagitalinei ašiai, pridėjimas užtikrina gerą šonkaulių sistemos aproksimaciją ir stuburo aplinkoje.

3. Pasiūlyta dviejų žingsnių optimizavimo strategija modelio parametrams rasti: pirmame žingsnyje sprendžiamas supaprastintas (mažesnio kintamųjų skaičiaus) uždavinys, po to optimizavime naudojami visi kintamieji. Parodyta, kad globaliojo optimizavimo problemai spręsti pakanka lokaliojo optimizavimo metodų.
4. Pasiūlytas registravimo metodas yra invariantiškas poslinkiui, posūkiui ir mastelio pokyčiui, todėl sluoksnius galima registruoti nepriklausomai nuo paciento pozicijos lovos atžvilgiu ir tomografo parametrų, lemiančių pikselių dydį. Pasiektas $\sim 0{,}1$ mm registravimo tikslumas.
5. Eksperimentai rodo, kad piramidiniu Lucas-Kanade algoritmu gauta transformacijos matrica netinkama pirminiam vaizdui transformuoti, nes dėl nedidelių pokyčių transformacijoje atsiranda didelių pokyčių registravimo rezultatuose: vidutinė paklaida yra 1 mm, o maksimali $-3{,}75$ mm. Geriausia su tais pačiais duomenimis pasiekta vidutinė paklaida – $0{,}33$ mm, o maksimali – $1{,}25$ mm.
6. Išbandytos keturios poslinkio invariantiškumo užtikrinimo strategijos ir trys mastelio pokyčio invariantiškumo strategijos. Geriausi rezultatai pasiekti, kai registruojama atsižvelgiant ne vien į šonkauliais apriboto kontūro formą, bet ir į kaulinį audinį vaizduojančių pikselių tankį atskirų modelio kreivės taškų aplinkoje – taip įvertinami modelio kreivės taškų svoriai. Svorių naudojimas leido gauti eile geresnį registravimo tikslumą lyginant su geriausiu nesvoriniu metodu.

Trumpai apie autorių

Mykolas J. Bilinskas Vilniaus universitete įgijo informatikos bakalauro (2011 m.) ir magistro (2013 m.) laipsnius. Baigus magistrantūros studijas už akademinius pasiekimus jam suteiktas Cum Laude diplomas. 2013–2017 m. studijavo informatikos krypties doktorantūrą Vilniaus universiteto Matematikos ir informatikos institute. 2009 m. pagal Erasmus mainų programą atliko praktiką Europos branduolinių tyrimų centre (CERN, Šveicarija). 2012 m. dirbo „Altechna R&D, UAB“, Vilniuje, programuotoju.

Mykolas Jurgis Bilinskas

DEVELOPMENT AND APPLICATION OF A MATHEMATICAL MODEL TO PARAMETRIZATION AND REGISTRATION OF BREAST AREA COMPUTED TOMOGRAPHY

Summary of Doctoral Dissertation
Physical Sciences
Informatics (09 P)

Editor Janina Kazlauskaitė

Mykolas Jurgis Bilinskas

MATEMATINIO MODELIO SUKŪRIMAS IR TAIKYMAS KRŪTINĖS LĄSTOS KOMPIUTERINĖS TOMOGRAFIJOS VAIZDAMS PARAMETRIZUOTI IR REGISTRUOTI

Daktaro disertacijos santrauka
Fiziniai mokslai
Informatika (09 P)

Redaktorė Jorūnė Rimeisytė